3-1-2019

A study of lightning flash initiation prior to the first initial breakdown pulse

Thomas Marshall
University of Mississippi

Sampath Bandara
University of Mississippi

Nilmini Karunarathne
University of Mississippi

Sumedhe Karunarathne
University of Mississippi

Ivana Kolmasova
Institute of Atmospheric Physics of the Academy of Sciences of the Czech Republic

See next page for additional authors

Authors

Thomas Marshall, Sampath Bandara, Nilmini Karunarathne, Sumedhe Karunarathne, Ivana Kolmasova, Raymond Siedlecki, and Maribeth Stolzenburg

A study of lightning flash initiation prior to the first initial breakdown pulse

Thomas Marshall[a,*], Sampath Bandara[a], Nilmini Karunarathne[a], Sumedhe Karunarathne[a,1], Ivana Kolmasova[b,c], Raymond Siedlecki[a], Maribeth Stolzenburg[a]

[a] *Department of Physics & Astronomy, University of Mississippi, University, MS 38677, USA*
[b] *Department of Space Physics, Institute of Atmospheric Physics CAS, Prague, Czechia*
[c] *Faculty of Mathematics and Physics, Charles University, Prague, Czechia*

ARTICLE INFO

ABSTRACT

This study examines the initiation of two intracloud (IC) and two cloud-to-ground (CG) lightning flashes using electric field change (FA) sensors and VHF (LogRF) sensors located at seven sites near Oxford, Mississippi, USA. For each flash the initiating event caused a pulse in the LogRF data and started an Initial E-Change (IEC) in the FA data. The initiating LogRF pulses had powers < 1 W and durations of ~1 μs. Numerous LogRF pulses occurred during each IEC; these pulses had durations ≤ 3 μs. Fewer FA pulses occurred during each IEC; these pulses had durations of ≤ 7 μs. During each IEC, a few of the LogRF pulses were coincident with a FA pulse, and most such pairs of pulses enhanced the IEC; no IEC enhancing events occurred without such a coincident pair. Each flash had 1 or 2 IEC enhancing events soon after the initiating event and 1 or 2 enhancing events shortly before the first classic initial breakdown (IB) pulse occurred. The point dipole moments and durations of IECs of the two IC flashes were (–520 C m, 620 μs) and (–770 C m, 1790 μs) and for the two CG flashes were (9 C m, 124 μs) and (36 C m, 130 μs). We speculate that the LogRF events were positive corona streamers, that enhancing events occurred when a new streamer extended a previous streamer path, and that this process during the flash initiation developed a nascent channel needed for the negative breakdown of the IB pulses.

1. Introduction

Until recently, lightning initiation has been thought to begin with initial breakdown pulses (IB pulses), as detected with electric field change (E-change) sensors operating in the VLF/LF/MF radio bands (e.g., Clarence and Malan, 1957; Kitagawa and Brook, 1960; Weidman and Krider, 1979; Bils et al., 1988; Nag et al., 2009; Marshall et al., 2013). IB pulses have also been called preliminary breakdown pulses, PB pulses, B pulses, and characteristic pulses. Weidman and Krider (1979) studied larger amplitude IB pulses and found that that they tended to be bipolar in shape and often had "two or three narrow, fast-rising pulses superimposed on the initial half cycle" of the bipolar shape. These larger IB pulses are referred to as "classic" IB pulses herein, and the fast-rising pulses are termed "subpulses." Weidman and Krider (1979) determined that classic IB pulses of cloud-to-ground (CG) lightning flashes and of intracloud (IC) flashes had durations averaging 41 μs and 63 μs, respectively, with ranges of 10–100 μs and of 10–230 μs, respectively. Using a high speed video camera operating at 50,000–54,000 frames/s and an array of E-change sensors, Stolzenburg

et al. (2013) showed that bursts of light were coincident with classic IB pulses of CG and IC flashes; for seven CG flashes with the IB pulses in the field of view of the camera, the IB pulses developed as a thin, linear "initial leader" that visibly extended with each IB pulse to lengths of 300–1500 m. Using an E-change sensor with a bandwidth of 16 Hz – 10 MHz and a sampling interval of 4 or 10 ns, Nag et al. (2009) studied 12 CG and 12 IC flashes and found that the majority of the pulses during the IB stage of the flashes "were relatively small in amplitude and duration" compared to classic IB pulses. Nag et al. (2009) called these more numerous pulses "narrow" pulses; in one flash 26% of the narrow pulses had durations < 1 μs. Stolzenburg et al. (2014) showed that narrow IB pulses were often associated with new, relatively dim luminosity acting as precursor events to classic IB pulses. The physical mechanisms that produce narrow and classic IB pulses are still unknown.

In studying the initiation of 18 CG lightning flashes and 18 IC lightning flashes, Marshall et al. (2014) found that an Initial E-Change (an "IEC") preceded the first IB pulse. Furthermore, Marshall et al. (2014) found an impulsive event was coincident with the beginning of
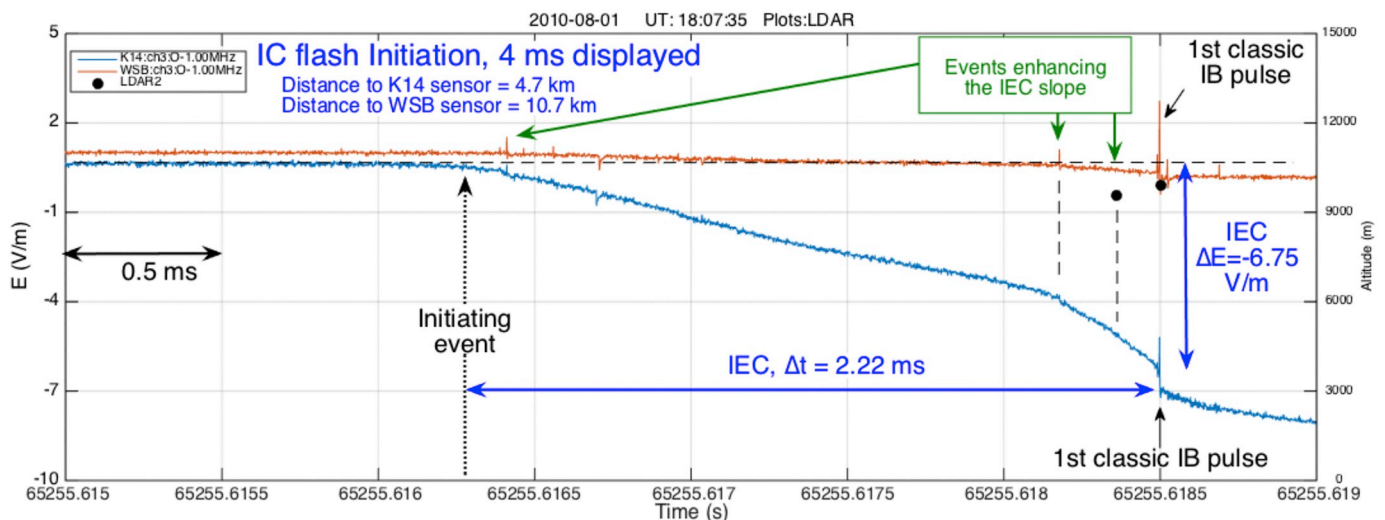

Fig. 1. Example of an IEC in an intracloud flash [after Fig. 1b from Chapman et al., 2017] showing 4 ms of E-change data from two sensor sites (K14 and WSB) in Florida in 2010. The first VHF (LDAR2) event occurred at a horizontal range of 4.7 km from the K14 sensor and 10.7 km from the WSB site. The vertical arrow marked "Initiating event" indicates the time that the IEC began; there was neither a VHF event nor an obvious E-change pulse at the beginning of the IEC. The E-change of the IEC was −6.75 V/m and its duration was 2.22 ms. The E-change data have been time shifted to the occurrence location of the first LDAR2 event. Three "enhancing" events that increased the magnitude of the slope of the IEC are marked.

14 of the 36 IECs studied and suggested that this event was the real cause of the lightning initiation. The 14 impulsive initiation events were detected with a VHF lightning mapping array (LDAR2) at the NASA/Kennedy Space Center. Marshall et al. (2014) proposed a three-stage sequence of events for lightning initiation: (1) an impulsive event (the real initiating event) followed by (2) an IEC (duration 0.1–6 ms) followed by (3) the first (classic) IB pulse of the flash (10–60 μs duration). Marshall et al. (2014) noted that many IECs were enhanced (given a greater E-change slope with time) by additional events that seemed similar to the initiating event; herein we call these enhancing events. Fig. 1 shows the three-step sequence as seen in E-change data, including IEC enhancing events. In a follow-up study, Chapman et al. (2017) showed that all 75 lightning flashes in two thunderstorms had an IEC before the first IB pulse. Based on that finding, Chapman et al. (2017) suggested that the 75 flashes may have needed an IEC to start the IB pulses.

Using a VHF digital interferometer, a different VHF lightning mapping array (called LMA), and a single E-change sensor, Rison et al. (2016) showed that for many (and perhaps all) flashes, the first event of lightning initiation was caused by "fast positive breakdown," or FPB. Rison et al. (2016) stated that FPB was the impulsive event that Marshall et al. (2014) identified as initiating lightning flashes. Rison et al. (2016) defined FPB as consisting of a "volumetrically distributed system of positive streamers or streamer-like activity (Phelps, 1974; Griffiths and Phelps, 1976)" occurring in virgin air with limited extent (≤500 m) and fast speeds of $1–10 \times 10^7$ m/s. Rison et al. (2016) studied three IC flashes that were initiated by especially energetic FPB events called positive Narrow Bipolar Events (+NBEs). These +NBEs had VHF powers of ~50 dBW (deciBels relative to 1 watt), FPB durations of 6–12 μs, and FPB velocities of 4×10^7–10×10^7 m/s. (As seen with E-change sensors, NBEs are bipolar pulses with typical durations of 10–30 μs and typical amplitudes of 5–20 V/m range-normalized to 100 km (e.g., Willett et al., 1989).) Rison et al. (2016) found that for IC (CG) flashes, the initiating FPB moved downward (upward) in altitude while the following IB pulses moved upward (downward). Rison et al. (2016) extended their analysis of the lightning initiating events by using LMA sensors (VHF bandwidth of 60–66 MHz) to determine the VHF source power of 51 IC flashes and 25 CG flashes from one thunderstorm. Their IC initiating event powers ranged from −18 dBW to 53 dBW with about 40% of the initial powers < 0 dBW, while their CG

initiation event powers ranged from −23 to 29 dBW with about 70% of the initial powers < 0 dBW. Recently Krehbiel et al. (2017) reported "clear-cut instances" of NBEs caused by upward-moving fast negative breakdown (FNB). This finding prompted Krehbiel et al. (2017) to investigate the possibility that both FPB and FNB are caused by "coronal or ionization waves."

Herein we report the first results from a study of lightning initiation in thunderstorms that occurred in 2016 near Oxford, Mississippi, USA. Using data from a seven-station array, we compare the full waveforms from VLF/LF/MF E-change sensors (e.g., Marshall et al., 2014; Chapman et al., 2017) with full waveforms from VHF sensors for two IC flashes and two CG flashes. We focus on the IEC period, that is, the time from the initiating event to the first classic IB pulse, and we investigate the various breakdown events detected by these two complementary sensors.

2. Instruments and methods

To study lightning initiation, we deployed an array of sensors at seven sensor sites within 45 km of Oxford, Mississippi, USA. Fig. 2c shows the seven sites along with time-of-arrival (PBFA) lightning locations of IB pulses from two flashes; PBFA and the flashes are discussed later. At each site there were four different sensors called Slow Antenna, Fast Antenna (FA), dE/dt, and LogRF. Data from all four sensors were digitized, time-tagged to GPS (Global Positioning System, with one sigma average of < 2 ns), and recorded on computers at each site. Each sensor's data were recorded continuously at 10 kiloSamples/s and in triggered mode at 10 MegaSamples/s (MS/s). Triggers for all sensors at each site occurred whenever a floating threshold was exceeded in the FA data. For each trigger 400 ms of data were recorded for each of the four sensors; the 400 ms included 250 ms immediately preceding the trigger and 150 ms following the trigger. If the trigger threshold was exceeded again during the original 150 ms of post-trigger recording time, the post-trigger data collection was extended to 150 ms after the second trigger; a third trigger would extend the post-trigger data to 150 ms after the third trigger, etc. In this way, successive post-trigger extensions often resulted in a data record covering an entire flash even if the flash duration was much longer than 400 ms.

The study herein uses data from the Fast Antenna and LogRF sensors, described next. Details of the dE/dt and Slow Antenna sensors are

(a)

(b)

(c)

(d)
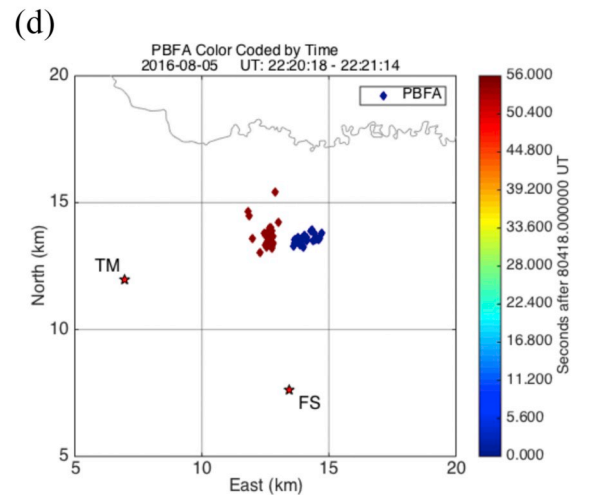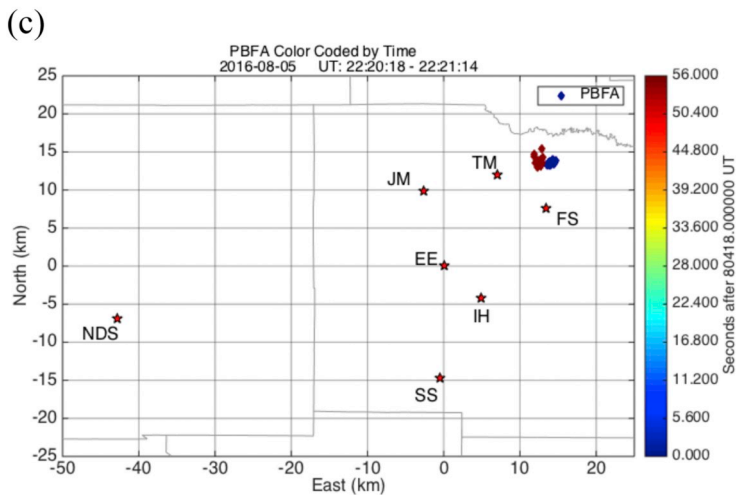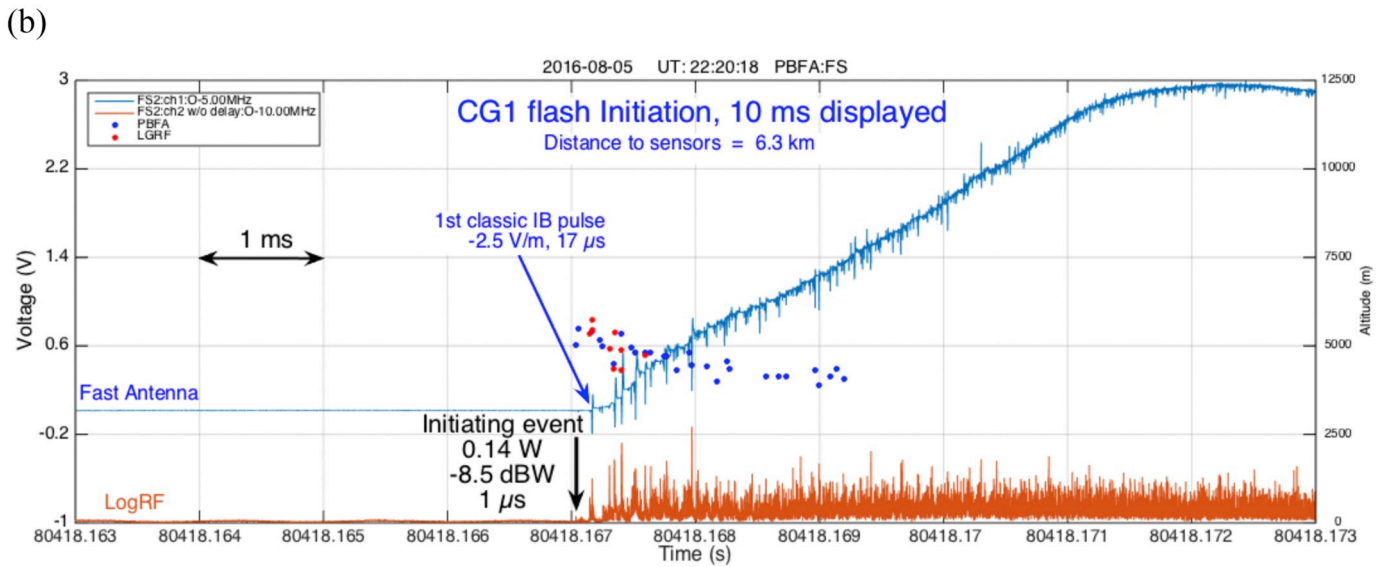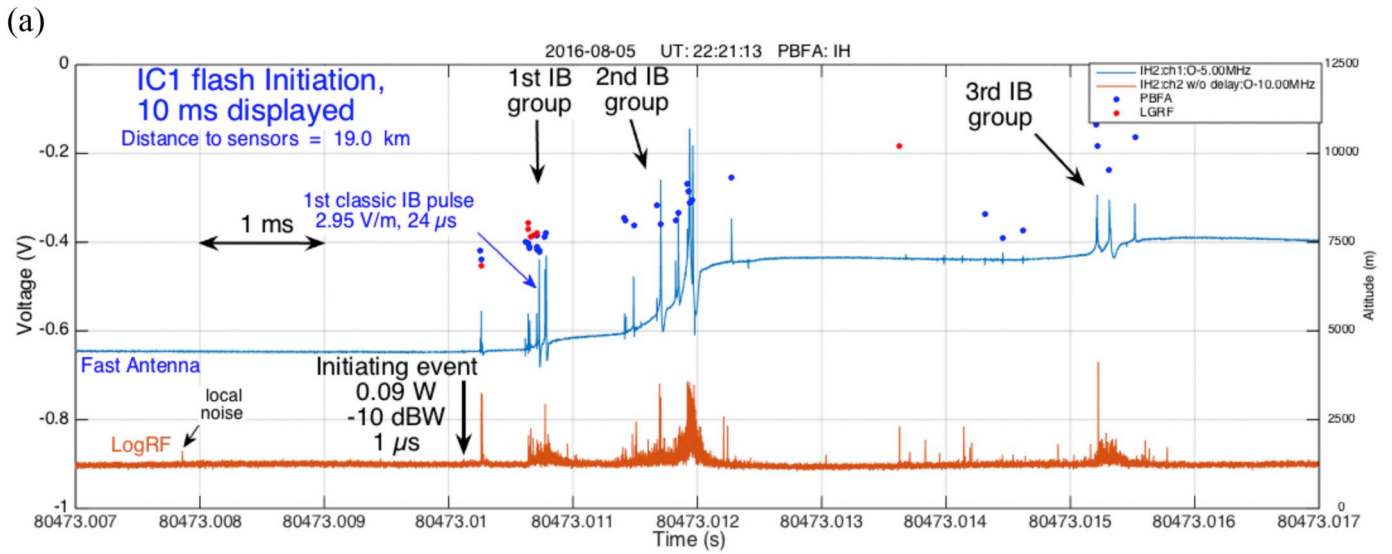
(caption on next page)

Fig. 2. (a) First 10 ms of lightning data of IC1, an IC flash on 5 August 2016 plotted versus time in seconds from midnight. Data from the IH sensors at a horizontal range of 19.0 km from the initiation events shown. The upper (blue) curve shows the Fast Antenna (FA) data (uncalibrated linear scale in volts, left axis); lower (red) LogRF curve shows VHF power (uncalibrated logarithmic scale in volts, left axis). PBFA locations of some FA pulses and LGRF locations of some LogRF pulses are plotted as altitude (right axis) versus event arrival time at the IH sensor. The initiation event along with its LogRF power and duration are indicated with an arrow. The first classic IB pulse along with its range-normalized amplitude (RNA, relative to 100 km) and duration are also shown. (b) Similar to (a), showing the first 10 ms of lightning initiation data (from the FS site) of CG1, a CG flash on 5 August 2016. (c) Horizontal PBFA locations for the IC flash (red diamonds) and for the CG flash (blue diamonds) are shown along with all seven of the 2016 sensor sites. (d) Expanded view of PBFA locations shown in (c). (For interpretation of the references to colour in this figure legend, the reader is referred to the web version of this article.)

given in the Appendix.

A. The Fast Antenna (FA) was a calibrated flat-plate E-change sensor with an electronic decay time of 10 ms, which is relatively long compared to most sensors with this name. The bandwidth was 16 Hz – 2.6 MHz, so the FA "characteristic length" (speed of light/frequency) of the electromagnetic waves detected was ≥120 m. Data were digitized at 10 MegaSamples/s (MS/s) with a bit depth of 12, then averaged to 5 MS/s and recorded. The FA can record, with essentially no electronic distortion, pulses with durations in the range 0.6 μs to > 250 μs. The FA can also detect IECs, but the net E-change is substantially undervalued for IEC durations > 4 ms. The E-change detected by the FA was caused by a rearrangement of charges; a static charge distribution has a zero field change. The charge rearrangement is due to charge motions that create a new charge distribution in the cloud. The E-change can be divided into three components called electrostatic, induction, and radiation (e.g., Clarence and Malan, 1957; Uman et al., 1975). Except for pulses close to a sensor, the E-change pulses are dominated by the radiation component.

Note that the FA measured the vertical component of electric field change but not the horizontal component. We can assume that the FA sensor was located at the surface of a flat, perfectly conducting plane (the Earth); this approximation is quite good since the FA sensor was 1–3 m above the ground and the moving charges were only 5–9 km above the ground, while the Earth's radius is approximately 6400 km and its conductivity is relatively large in Mississippi. With the flat ground assumption, one can use Gauss's Law and the method of images (a proxy for charge motions at the surface of the Earth) to show that there would only be a vertical component of electric field change for the FA to measure, regardless of the orientation of the charge motion in the cloud causing the electric field change. We note, however, that the finite conductivity of the Earth could lead to a horizontal electric field at the surface of the Earth that the FA does not measure; in the discussions below the reader should remember that the FA only measured the vertical component of electric field change.

B. The LogRF sensor was a VHF sensor to measure power in a logarithmic scale, with an effective range of approximately −75 dBm to −25 dBm (dBm = decibels relative to a milliwatt). Bandwidth was 186–192 MHz, so the characteristic length of the electromagnetic waves detected by LogRF was ≈ 1.6 m. Data were digitized and recorded at 10 MS/s with a bit depth of 12. With 10 MS/s sampling, the LogRF sensors can accurately record pulses with durations ≥0.4 μs. The LogRF sensors were calibrated following the method used by Hamlin (2004). Thus, if the range to the event is known, the source power of the event can be determined (e.g., Hamlin, 2004).

The seven-site array allows us to determine the location (x, y, z, t) of fast lightning events with each sensor type by using the time-of-arrival algorithm of Karunarathne et al. (2013). Locations determined from FA or slow antenna data are called "PBFA" locations as in Karunarathne et al. (2013). LogRF data can also be fed into the algorithm to yield "LGRF" locations. For lightning flashes that occurred near the sensor array, like the ones shown in Fig. 2, the PBFA and LGRF locations typically have estimated horizontal errors (Δx and Δy) < 400 m, altitude errors (Δz) < 400 m, and timing errors (Δt) ≤ 2 μs. For lightning

flashes that occurred within the sensor array, like the ones shown in Fig. 3, the PBFA and LGRF locations typically have estimated horizontal errors (Δx and Δy) < 100 m, altitude errors (Δz) < 200 m, and timing errors (Δt) ≤ 0.3 μs.

The fast electromagnetic pulses studied herein, with durations of 0.5–100 μs, are probably associated with electrical charge motions with lengths ranging approximately from 1 to 200 m (or more). Under the right conditions, any of these pulses might be detected by both FA and LogRF sensors. However, since the characteristic length of the VLF/LF/MF radiation detected by FA sensors was ≥120 m while the characteristic length of the LogRF radiation was about 1.6 m, we expect that pulses detected by the FA sensors were likely associated with much longer electrical charge motions than the pulses detected only by the LogRF sensors.

As mentioned above, the physical mechanisms that produce narrow and classic IB pulses are still unknown, making it difficult to precisely define or identify IB pulses. Classic IB pulses are known to move negative charge upward during the IB stage of typical IC flashes, downward during the IB stage of negative CG flashes, and downward in inverted IC flashes (Karunarathne et al., 2013; Chapman et al., 2017), but beyond that, little is known about the mechanism of classic IB pulses. Essentially nothing is known about the mechanism of narrow IB pulses. IB pulses have typically been observed with sensors similar to our Fast Antenna, and the identification as IB pulses was based on time of occurrence: FA pulses occurring during the first 5–10 ms of a flash were called IB pulses (e.g., Weidman and Krider, 1979; Nag et al., 2009; Karunarathne et al., 2013). However, the discovery of the IEC that precedes the first classic IB pulse (Marshall et al., 2014b, Chapman et al., 2017) raises the following question: "During the IEC are the FA pulses that occur IB pulses or not?" Another way of posing this question: "Is the first classic IB pulse the first IB pulse in a flash?" Until we know the mechanisms causing narrow IB pulses, classic IB pulses, and the FA pulses occurring during the IEC, we see no way of deciding if FA pulses occurring during the IEC are IB pulses or not. For this reason, in this work we will call pulses occurring during the IEC merely "FA pulses."

As described in the Introduction, classic IB pulses have been detected by numerous investigators, so defining their FA waveforms is straightforward. We define a classic IB pulse as having a bipolar waveform with a duration ≥10 μs and a relatively large amplitude; classic IB pulses often have subpulses on the leading part of the bipolar waveform (Weidman and Krider, 1979). This definition allows us to identify the first classic IB pulse of a flash. By definition, the first classic IB pulse marks the end of the IEC.

We use the physics convention for electric field polarity, which was described in Marshall et al. (2014) as "the direction of the electric field at a particular location is the same as the direction of the electric force on a positive test charge placed at that location."

3. Data and analyses

In this study we describe in detail the initiation of two IC flashes (IC1 and IC2) and two negative CG flashes (CG1 and CG2). The IC flashes were typical in the sense that they initiated at mid-level in the thundercloud and moved negative charge upward. Likewise, the negative CG flashes were typical in the sense that they initiated at lower

(a)

2016-08-26   UT: 17:53:08   PBFA: IH

IC2 flash Initiation
10 ms displayed

Distance to sensors = 8.9 km

1st classic IB pulse
-0.99 V/m, 13 μs

1st IB group

2nd IB group

1 ms

Fast Antenna

Initiating event
0.54 W
-2.7 dBW
1 μs

LogRF

- IH2:ch1:O-5.00MHz
- IH2:ch2 w/o delay:S-5.00MHz ×0.4
- PBFA
- LGRF

(b)

2016-08-26   UT: 17:51:26   PBFA:EE

- EE2:ch1:O-5.00MHz
- EE2:ch2 w/o delay:O-10.00MHz
- PBFA

CG2 flash Initiation, 10 ms displayed

Distance to sensors = 3.4 km

1st classic IB pulse
-0.32 V/m, 15 μs

1 ms

Initiating event
0.64 W
-1.9 dBW
2 μs

LogRF

Fast Antenna

(c)

PBFA LGRF Color Coded by Time
2016-08-26   UT: 17:53:08.4975 - 17:53:08.5001

- PBFA
- LGRF

milli seconds after 64388.497500 UT

EE

IH

(d)

PBFA LGRF Color Coded by Time
2016-08-26   UT: 17:51:26.3177 - 17:51:26.31815

- PBFA
- LGRF

micro seconds after 64286.317700 UT

EE

IH

(caption on next page)

14

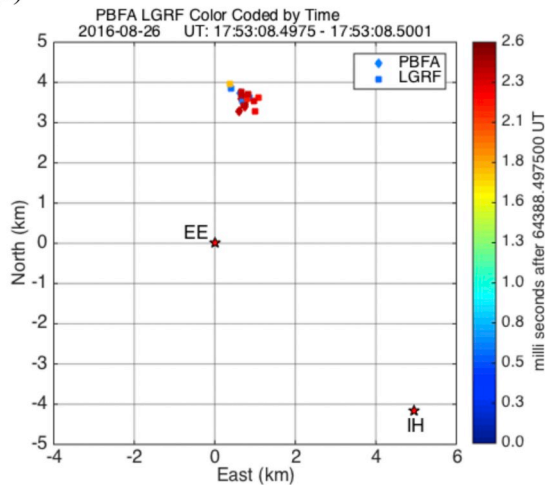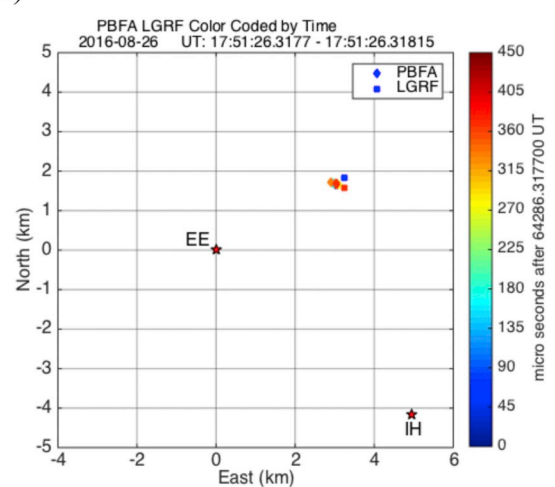**Fig. 3.** (a) Similar to Fig. 2, showing overview of lightning initiation data of IC2, an IC flash on 26 August 2016 plotted versus time in seconds from midnight. (b) Similar to Fig. 2, showing the first 10 ms of lightning initiation data of CG2, a CG flash on 26 August 2016. (c) Horizontal PBFA locations for the IC flash. (d) Horizontal PBFA locations for the CG flash.
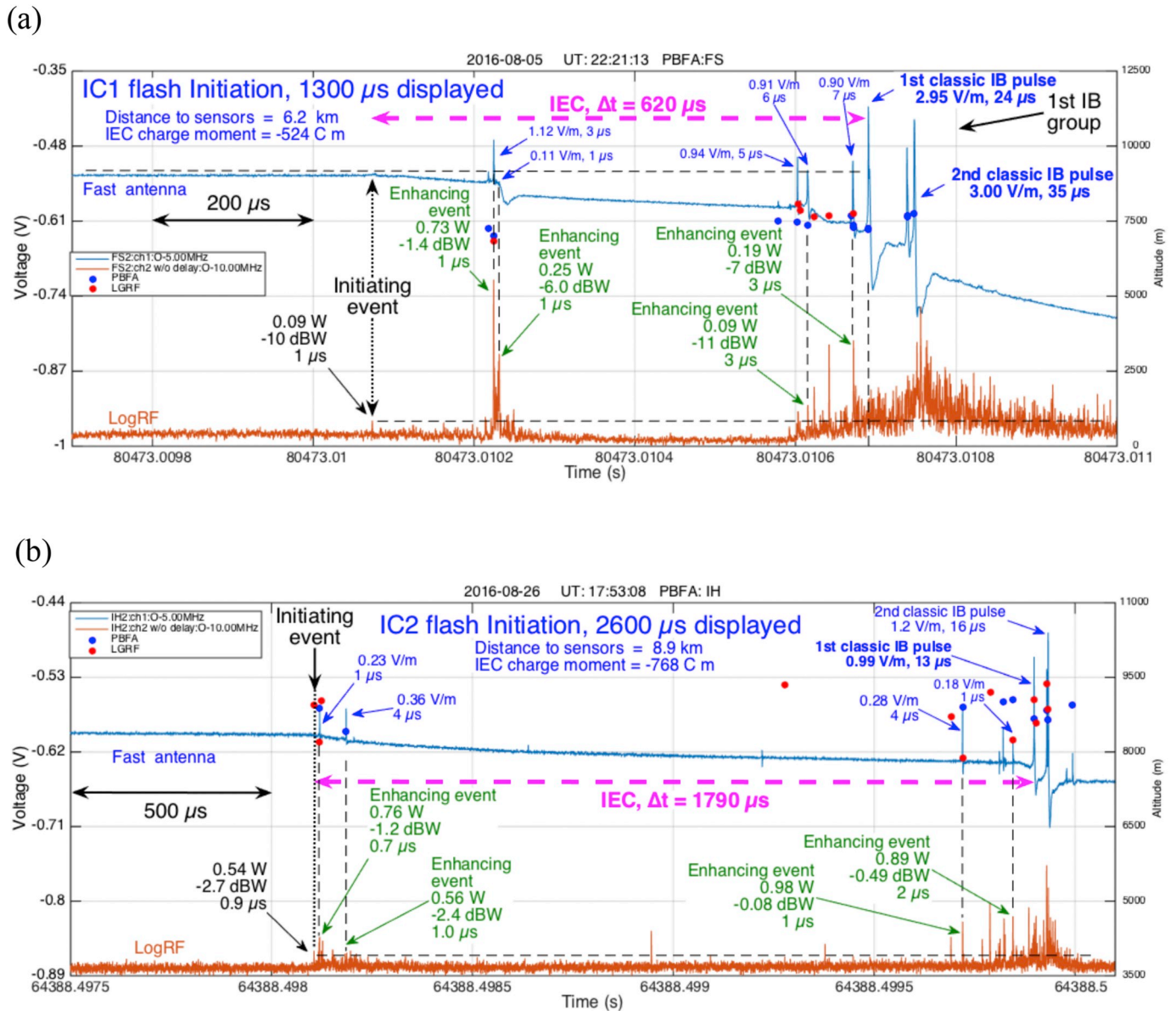

(a)

(b)

Fig. 4. Expanded views of IC flash initiations: (a) IC1 from Fig. 2a. (b) IC2 from Fig. 3a.

altitudes and moved negative charge downward. Fig. 2a and b show the first 10 ms of data from IC1 and CG1, both of which occurred on 5 August 2016; the flashes initiated within one minute and within 2 km horizontally of each other (see Fig. 2c and d). The flash initiations shown in Fig. 2 are typical of flashes recorded in our 2016 measurements in Mississippi thunderstorms. With one exception, the first several milliseconds in Fig. 2a and b show that there was essentially no electrical activity detected by either sensor before each flash initiation. The exception is a LogRF pulse about 2.3 ms before the IC1 flash initiation; this pulse is labeled as "local noise" since it was not seen by the other six LogRF sensors. As seen from the PBFA and LGRF event altitudes, the IC1 flash (Fig. 2a) initiated near 7.1 km altitude and developed upward. In IC1 the IB pulses occurred in temporal groups, as found by Marshall et al. (2013). PBFA and LGRF event altitudes indicate that the CG1 flash (Fig. 2b) initiated near 5.1 km and developed downward without any noticeable temporal grouping of IB pulses.

Based on the PBFA altitudes, the electrostatic reversal distances were 9.6 km for IC1 and 6.8 km for CG1. (For a review of reversal distance, see Rakov and Uman (2003, p. 71).) For IC1 (Fig. 2a) the FA data show positive electrostatic offset associated with each group of IB pulses, similar to the IC flashes studied by Marshall et al. (2013). Since IB pulses of typical IC flashes move negative charge upward (e.g., Shao and Krehbiel, 1996; Karunarathne et al., 2013) and since the FA sensor was beyond the electrostatic reversal distance, positive electrostatic offset is expected. For CG1 (Fig. 2b) the FA data also show positive electrostatic offset associated with the CG IB pulses, which are known to move negative charge downward (Karunarathne et al., 2013). The positive electrostatic offset fits with the fact that the FA sensor was within the reversal distance of the IB pulses of CG1.

Fig. 3 shows a 10-ms comparison of an IC flash initiation and a CG flash initiation from 26 August 2016; these flashes initiated within two minutes and 3 km horizontally of each other as shown in Fig. 3c and d.

The IC2 flash (Fig. 3a) developed upward from 9.2 km altitude and the CG2 flash (Fig. 3b) developed downward from 5.6 km altitude. In IC2 the IB pulses occurred in temporal groups, as also found for IC1. Based on the PBFA altitudes, the electrostatic reversal distances were 13 km for IC2 and 7.9 km for CG2, so the FA sensors were well within the reversal distance of both.

4. Overview: the first 10 ms of lightning initiation

On the basis of the data in Figs. 2 and 3 for IC and CG flash initiations, we can briefly highlight several observations. Perhaps most obvious is the finding that for both IC and CG flash initiations there are many more LogRF pulses than FA pulses. We had not expected to see so many LogRF pulses. This finding indicates there are many breakdown events with scales on the order of 1.6 m and comparatively few events with scales on the order of 120 m during the first 10 ms of both types of flashes.

The second and third general observations we note are not new, rather they support earlier work. As discovered by Kitagawa and Brook (1960), the FA data in Figs. 2 and 3 clearly show that IB pulses occur much less frequently in IC flashes than in CGs. Also, as found by Marshall et al. (2013), the FA data in Figs. 2a and 3a clearly show that the IB pulses of IC flashes occur in temporal groups with successive groups reaching successively higher altitudes.

Some other new findings are also clear from Figs. 2a and 3a: each group of IB pulses in IC1 and IC2 was accompanied by a burst of LogRF pulses, and relatively few LogRF and FA pulses occurred in the time intervals between the IB pulse groups. Although the IB pulses of CG1 and CG2 (Figs. 2b and 3b) did not occur in temporal groups, there was a burst of LogRF pulses at the time surrounding each IB pulse. These bursts are easy to see in CG2 because the IB pulses were not as closely spaced in time. The FA sensor in Fig. 3b was close to CG2, so the IB pulses included electrostatic offsets that caused a stair-step behavior in the FA data. Note that each stair-step (IB pulse) was accompanied by a "hill" of many LogRF pulses. Later figures will show the LogRF hills or bursts more clearly and will also show that these LogRF pulses typically had durations of 1–2 μs.

5. Initiation through the first classic IB pulse for IC flashes

Fig. 4a and b show expanded views of IC1 and IC2 from just before initiation through the first group of classic IB pulses. For larger FA pulses the pulse amplitude, range normalized to 100 km, and the pulse duration are shown; the amplitudes were determined using a more distant sensor unaffected by the electrostatic and induction components of the E-change. The VHF source power and duration of several LogRF pulses are also shown.

5.1. Initiating event of IC flashes

To identify the initiating event of IC1 and IC2 in Fig. 4a and b we used both FA and LogRF data. (Note that in Fig. 4b the altitude scale for LGRF and PBFA is 3500 m – 11,000 m to accentuate the LGRF altitudes discussed later.) Fig. 5a and b show expanded views (400 μs) that include the initiating event for IC1 and IC2. For both flashes the FA data clearly show the negative slope of the IEC, and the initiating event occurred at the beginning of the IEC. No distinct FA pulse was observed at the time of the initiating event in either flash; apparently the charge motions of the initiating event were too short in length and/or too weak in charge to be detected with the FA. In both flashes the first LogRF pulse above background was coincident with the beginning of the IEC. In both flashes the first LogRF pulse was relatively weak, 0.09 W (-10 dBW) and 0.54 W (-2.7 dBW), compared to initiating events for 51 IC flashes in Rison et al. (2016) (described above). Since positive corona streamers occur in a smaller electric field (reduced by a factor of 4 or 5) than negative corona streamers (e.g., Phelps, 1971), we infer the

initiating event of both IC flashes, as detected with the LogRF sensor, was one or more positive corona streamers. (Note, however, that streamer polarity cannot be determined from the LogRF data). Based on the findings of Rison et al. (2016), we might further infer that the positive corona streamer event was FPB. However, we have no way of determining the streamer speed, so we cannot know if they were "fast" ($\sim 5 \times 10^7$ m/s) as defined by Rison et al. (2016). We can state that the initiating event of each flash lasted ~1 μs in the LogRF data, much shorter than the durations of 6–14 μs for FPB initiating events of IC flashes investigated by Rison et al. (2016).

5.2. IECs of IC flashes

During the IECs of IC1 and IC2 (Fig. 4a and b), the overall electric field change was negative, with point dipole charge moments of –520 C m and -770 C m, respectively. (The method of calculating the point dipole moment is described in Marshall et al. (2014).) For 46 IC flashes studied by Chapman et al. (2017), the average point dipole moment of the IECs was –140 C m with a range of -8 to –650 C m. Thus the charge moments of IC1 and IC2 in Fig. 4 are relatively large; this fact may indicate that the thundercloud electric field in the vicinity was not close enough to the value needed to cause the negative breakdown associated with classic IB pulses. The reasoning behind this indication is as follows. First, we assume that the thundercloud's electric field (a negative vertical field for IC flash initiation) was initially not sufficient to cause a classic IB pulse because a classic IB pulse did not occur until the end of the IEC. Second, we assume that during the IEC the cloud electric field moved the charges that were freed during the initiating events; the charge motion was vertically downward for free positive charges and upward for free negative charges. The charge motion created a simple dipolar charge distribution that reduced the electric field between the dipolar charges and increased the negative electric field above the upper dipolar charge (due to the superposition of the cloud electric field and the dipolar electric field). When the negative electric field was big enough, the first classic IB pulse occurred and moved negative charge upward. Thus, since these IEC dipole moments were large, then the cloud electric field must have been smaller than needed to cause a classic IB pulse.

During the IECs of IC1 and IC2 (Fig. 4a and b), there were 7 and 8 (respectively) noticeable FA pulses. The FA pulses had short durations ($\leq$ 7 μs), relatively small amplitudes ($<$ 25% of the largest IB pulse amplitude), and smooth bipolar or unipolar waveforms. Also during the IECs of IC1 and IC2, there were roughly 40 and 20 (respectively) large-amplitude LogRF pulses, with amplitude $\geq$ the amplitude of the initiating LogRF event. (The amplitude of the initiating event is indicated by a horizontal dashed line in the figures.) All of the large-amplitude LogRF pulses had short durations ($\leq$ 3 μs).

For IC1 and IC2, the FA and LogRF pulses located by PBFA or LGRF were tightly clustered in horizontal location (see Figs. 2d and 3c). Although they were not all locatable, it is likely that the other FA and LogRF pulses that occurred during the IEC were also associated with these two IC flashes.

The downward sloping IEC seen immediately after initiation in the FA data of IC1 and IC2 (Figs. 4 and 5) indicates that the initiating event started the IEC electric field change, ΔE. Presumably the positive corona streamer(s) of the initiating event created a weak plasma with mobile charges. Dawson and Winn (1965) modeled a positive corona streamer as a sphere of positive charge, replicating itself as it moved forward via avalanches ahead of the sphere. Phelps (1974) noted that such a positive corona streamer would leave behind a trail with more negative ions than positive ions. Thus the earliest part of ΔE of the IEC was probably caused by the motion of the free charges in the weak plasma, with positive charges moving downward and negative charges moving upward. The path of such a positive corona streamer would constitute a nascent channel having weak conductivity.

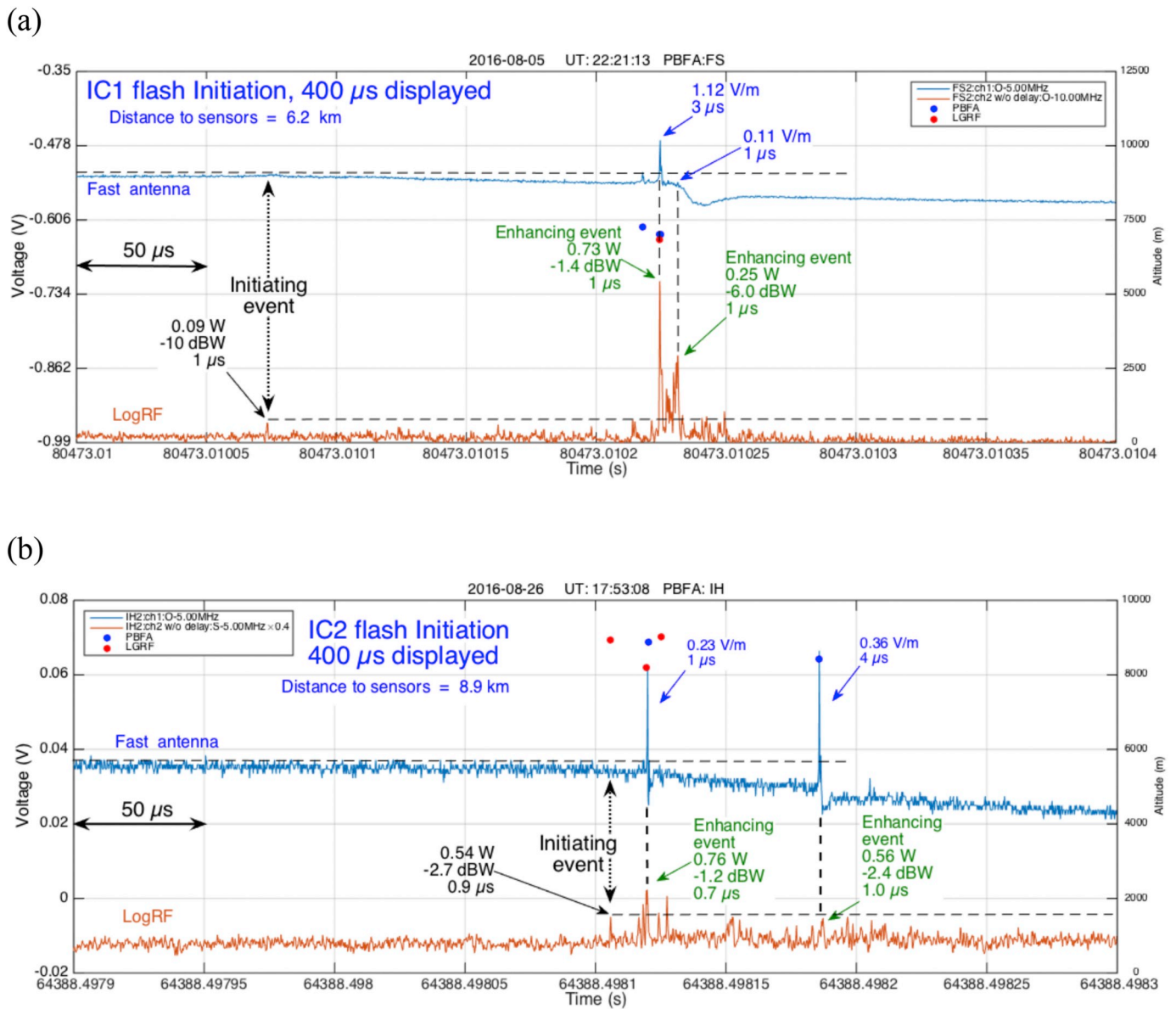These early charge motions in the IEC would create a small vertical

(a)

(b)

Fig. 5. Expanded views (400 μs) FA and LogRF data showing the initiating event and the first enhancing events for IC flash initiations: (a) IC1. (b) IC2.

dipole that would, in turn, increase the electric field above and below the dipole, as described above. Eventually, the increasing field would start additional positive corona streamers, as suggested by Phelps (1974) and Griffiths and Phelps (1976). Fig. 5 shows that IC1 and IC2 each had a pair of enhancing events soon after the initiating event (149 μs and 15 μs after initiation in Fig. 5a and b, respectively). The first enhancing event in IC1 lasted only 4 μs before the next enhancing event occurred, while the first two enhancing events in IC2 were separated by 65 μs. Both early enhancing events of each flash increased the downward slope of each IEC. Based on Phelps (1974) and Griffiths and Phelps (1976), we suspect that these events were additional positive corona streamers moving downward. The enhancing events had LogRF powers ≥ the LogRF power of the initiating event. Unlike the initiating event, however, there was a noticeable coincident FA pulse with each enhancing event. In each flash there was a series of relatively large amplitude LogRF pulses leading up to each of the two enhancing events, so it seems possible that each LogRF pulse was caused by an individual positive corona streamer or small system of such streamers. We hypothesize that an FA pulse coincident with an enhancing positive streamer occurred because the streamer began at the end of the nascent

channel associated with the initiating event, and thereby extended the nascent channel and made it more conductive. Another possibility is that an enhancing event connects two or more previous positive streamers. In either case the FA pulse would have been caused by current moving through a longer, weakly conductive nascent channel. Alternatively, these LogRF events could have been caused by negative breakdown from the upper end of the nascent leader, as found by Rison et al. (2016) during the IEC following their +NBE2. However, this cause seems less likely for IC1 and IC2 because the net increase in electric field due to these small dipoles seems insufficient to start negative breakdown (unlike the electric field increase after the large dipole caused by +NBE2 of Rison et al. (2016)).

After the two early enhancing events seen in IC1 and IC2, both IECs continued to have an approximately constant downward slope in the FA data for ~200 μs and ~1500 μs (respectively) even though there were only a few noticeable pulses detected by the FA or LogRF sensors. This steady slope may have been caused primarily by charge motion within the nascent weakly ionized channel driven by the thundercloud electric field.

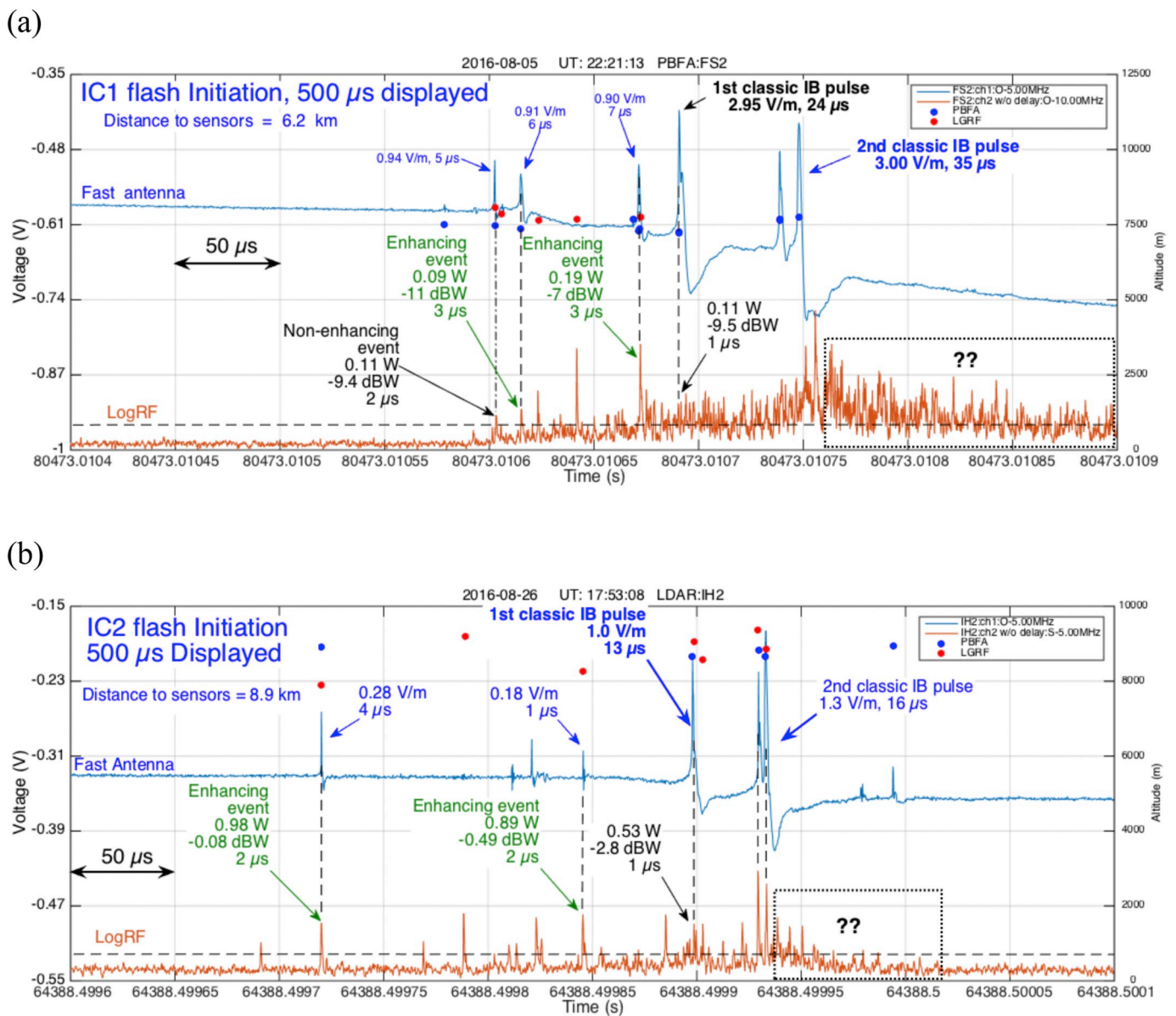Fig. 6 shows an expanded view (500 μs) of the end of the IEC for IC1

(a)

(b)

Fig. 6. Expanded views (500 μs) FA and LogRF data leading up to and including the first two classic IB pulses of the IC flash initiations: (a) IC1. (b) IC2. In each plot a dotted rectangle with double question marks outlines a large number of LogRF pulses of unknown origin.

and IC2. This time period includes the first classic IB pulse group of each flash (see Figs. 2a and 3a). Just before the first classic IB pulse IC1 and IC2 each had two enhancing events that caused increases in the downward slope of the IEC with time. Both enhancing events had LogRF powers ≥ the LogRF power of the initiating event and had noticeable coincident FA pulses. In this time period just before the first classic IB pulse there were also many LogRF pulses without coincident FA pulses; these LogRF pulses had short durations of 1–3 μs. These LogRF pulses could have been caused by positive corona streamers or could have been caused by some sort of negative breakdown (e.g., Rison et al., 2016; Krehbiel et al., 2017). Also highlighted in Fig. 6a is a coincident pair of FA and LogRF pulses in IC1 that did not cause a noticeable enhancement to the IEC, marked in Fig. 6a as a "non-enhancing" event. We do not know if the lack of a detected IEC enhancement was due to no enhancement occurring or to only a very weak enhancement or to any weak enhancement being obscured by the enhancing event that occurred just 12 μs later.

Because IC2 was near the center of the sensor array and at a relatively high altitude, IC2 yielded LGRF locations with especially small

errors (< 50 m in each horizontal dimension and approximately 100 m in altitude) and is thus worthy of close examination. In this case it can be seen in Fig. 4b that the three enhancing events with LGRF locations had the lowest altitudes (by at least 700 m) of all the LGRF events in the IEC of IC2. The first LGRF enhancing event occurred 15 μs after the initiating event at an altitude 740 m lower than the initiating event (Fig. 5b). The second LGRF enhancing event occurred 31 μs after the previous LGRF pulse and was 820 m lower than that previous LGRF pulse (Fig. 6b). The third LGRF enhancing event occurred 57 μs after the previous LGRF pulse and was 960 m lower than that previous LGRF pulse (Fig. 6b). The enhancing events were horizontally displaced from the previous LGRF pulses by 300–500 m, but all three enhancing events were located horizontally within a circle with a radius of 150 m. Thus the LGRF location data support the notion that enhancing events may have extended the nascent positive corona channel farther downward.

Overall, during the IECs of IC1 and IC2 there were many more large-amplitude LogRF pulses than narrow IB pulses in the FA data, so most of the large-amplitude LogRF pulses were not coincident with a noticeable FA pulse. A few of the noticeable FA pulses were not associated with a

large-amplitude LogRF pulse. Overall, the most noteworthy correlation between FA pulses and LogRF pulses was that all of the enhancing events had a coincident pair of noticeable FA pulse and large-amplitude LogRF pulse.

5.3. The first classic IB pulses of IC flashes

The FA data of Fig. 6 shows the first two classic IB pulses of IC1 and IC2. The first classic IB pulse of both flashes was a simple bipolar pulse without subpulses on the rising side. Both first IB pulses had relatively small LogRF powers: only 0.11 W (−9.5 dBW) and 0.53 W (−2.8 dBW). The LogRF powers were somewhat larger in the second classic IB pulse of each IC flash. Fig. 6 also provides a better view of the numerous large-amplitude, short-duration LogRF pulses that occurred during the first two classic IB pulses, comprising the LogRF bursts or hills mentioned above. Two other features of these IC flashes should be noted in Fig. 6. Firstly, in both IC1 and IC2 the second classic IB pulse occurred soon after the first, and each second IB pulse had a single large subpulse on the rising side of the bipolar pulse. Although we have found a few other IC flashes with similar first and second classic IB pulses (a simple bipolar IB pulse followed by a bipolar IB pulse with a single large subpulse), this pairing is not especially common for IC flashes in our data. Secondly, in both IC1 and IC2 the second classic IB pulse was followed by an almost continuous series of large-amplitude LogRF pulses having almost no coincident FA pulses (outlined in Fig. 6a and b with a dotted rectangle and double question marks): these LogRF pulses were part of the hill or burst of LogRF pulses associated with each IB pulse, discussed in Section 4. We do not know the cause of these LogRF pulse series.

5.4. Summary: initiation through the first classic IB pulse for IC1 and IC2

One important finding of the above detailed analysis is that the initiating event of IC1 and IC2 is weaker in LogRF power than many of the other events that occur during the IEC. Another important finding is that the enhancing events during the IEC have a noticeable coincident pair of FA/LogRF pulses and usually the LogRF pulse is more powerful than the initiating event. However, one coincident pair of FA/LogRF pulses did not cause a detected IEC enhancement. Overall, the initiating events of the IC1 and IC2 flashes in Fig. 4 were probably positive corona streamers moving downward, emitting weak VHF powers (five orders of magnitude weaker than the strong +NBE-initiated IC flashes studied by Rison et al. (2016)). After the initiating events, enhancing events during the IEC helped increase the electric field at the ends of the nascent channel and helped increase the conductivity of the nascent channel. We hypothesize that the enhancing events were also positive corona streamers moving downward from the lower end of the nascent leader, but we cannot rule out negative breakdown from the upper end of the nascent leader. The locations of the LogRF pulses in IC2, closely examined and described above, lend some support to the idea that enhancing events were caused by positive corona streamers moving downward from the lower end of a previous corona streamer. We further hypothesize that increased electric field and increased channel conductivity during the IEC were needed to start the negative breakdown of the first classic IB pulse, which moved upward from the upper end of the nascent leader.

6. Initiation through the first classic IB pulse for CG flashes

Rison et al. (2016) showed two examples of CG flashes with FPB moving upward at initiation while the IB pulses moved downward (opposite of IC flashes). Marshall et al. (2014) determined that IECs of CG flashes have a positive slope (opposite of IC flashes). Chapman et al. (2017) found that the average IEC duration of 17 CG flashes was 230 μs, an order of magnitude shorter than in IC flashes. They also found that the average IEC point dipole moment of 14 CG flashes was 26C m, a

factor of 5 smaller than in IC flashes. However, the shortest IEC durations and smallest IEC point dipole magnitudes were about the same for IC and CG flashes (Chapman et al., 2017).

Fig. 7a and b show expanded views of CG1 and CG2 (Figs. 2b and 3b) from just before initiation through the first classic IB pulse. Because the CG initiations occur much lower (near 5 km altitude in these cases) than the IC1 and IC2 flash initiations, the reversal distances are shorter and it is more difficult to have a sensor appropriately located to detect the IECs of CG flashes. Furthermore, for the IEC of CG1 the horizontal distance from the nearest sensor to the IEC was 6.3 km while the reversal distance was 6.8 km, so one would expect the IEC (essentially an electrostatic field change) to be fairly small since the electrostatic component is zero at the reversal distance. For this reason Fig. 8 is included to better show the IEC of CG1.

6.1. Initiating events of CG flashes

As in the IC flashes, we identified each initiating event of CG1 and CG2 as the first LogRF pulse above background. The initiating LogRF event for CG1 (Fig. 7a) had a power of 0.14 W (−8.5 dBW) and a duration of 1 μs, while the initiating event for CG2 (Fig. 7b) had a power of 0.64 W (−1.9 dBW) and a duration of 2 μs.

The identifications of the two initiating events are mainly supported by the IEC detected in the FA data. For the initiation of CG1, Fig. 8a shows that the IEC began close to or at the time of the first LogRF pulse above background. Based on Fig. 8b, there was no FA pulse coincident with the CG1 initiating event, which was also true for the IC flash initiating events discussed above. However, the data in Fig. 8b indicate that the CG1 initiating event was followed in 3 μs by the first enhancing event, and it is not clear if the IEC began precisely at the time of the first LogRF pulse or 3 μs later. For CG2, the IEC was detected in the FA data at the EE site and started at the time of the first LogRF pulse above background (Fig. 7b) which we identify as the initiating event.

Unlike the initiating events of the IC1, IC2, and CG1 flashes (Figs. 4a, b, 7a), there was a noticeable negative FA pulse coincident with the initiating event of CG2 (Fig. 7b). We can assume that the FA pulse is a weak negative NBE caused by upward-moving FPB, as described in Rison et al. (2016). For comparison, Chapman et al. (2017) investigated all the flashes in two thunderstorms (17 CG flashes, 55 IC flashes, and 3 inverted IC flashes) and found a noticeable FA pulse coincident with the beginning of the IEC in 21 cases (28% of the flashes).

Similar to the IC flashes, we infer that the initiating event of CG1 was a positive corona streamer or streamers and that the initiating event of CG2 was a system of positive streamers (the FPB of the weak negative NBE). The initiating events of CG1 and CG2 are quite similar in power and duration to those in IC1 and IC2 discussed above. The event powers in the VHF are also similar to the CG initiation powers reported by Rison et al. (2016). However, the CG1 and CG2 LogRF initiating event durations (1–2 μs) were much shorter than the durations of 6–14 μs reported by Rison et al. (2016).

6.2. IECs of CG1 and CG2

The IEC of CG1 (Fig. 7a and expanded in Fig. 8) had a duration of 130 μs with a positive slope and a point dipole charge moment of 36C m, making it typical of IECs in CG flashes (e.g., Chapman et al., 2017). The IEC was also similar to IECs of IC1 and IC2 studied above in several ways. Firstly, there were two early enhancing events (separated by only 19 μs) and one late enhancing event, all enhancing events had powers ≥ the initiating event power, and all had noticeable coincident FA pulses. Secondly, there were more LogRF pulses than FA pulses. Thirdly, there was a relatively long interval of about 60 μs in the middle of the IEC where the slope of the IEC remained approximately constant. Finally, the number and magnitude of LogRF pulses increased shortly before the first classic IB pulse. The main difference was that the IEC of
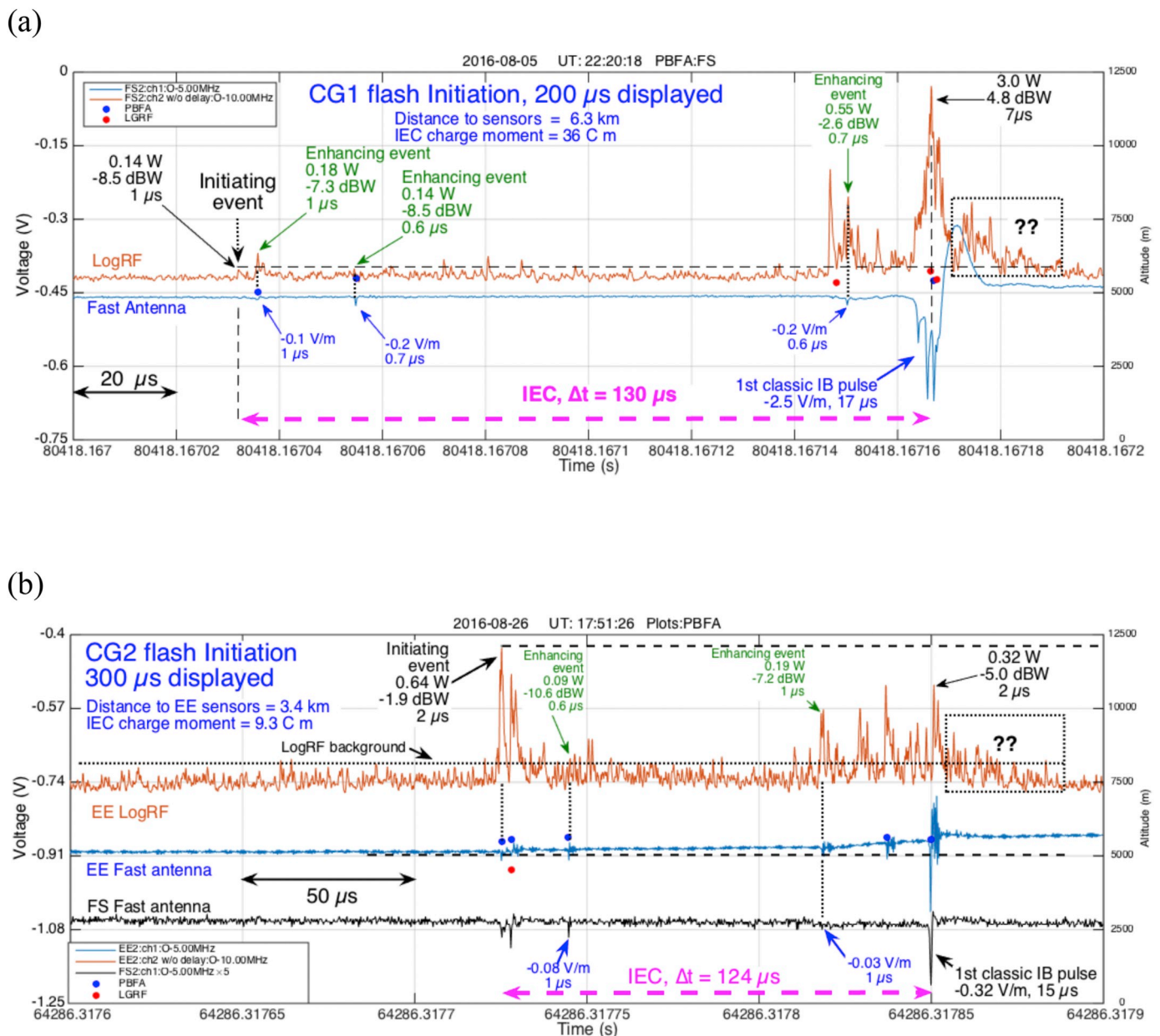
(a)

(b)

Fig. 7. Expanded views of CG flash initiations. (a) First 200 μs of CG1 from Fig. 2b. (b) First 300 μs of CG2 from Fig. 3b. Since the LogRF background was noisier at the EE site than at other sites, a dotted line is included to show the approximate background level. In each plot a dotted rectangle with double question marks outlines a large number of LogRF pulses of unknown origin.

CG1 had no noticeable FA pulses without LogRF pulses, unlike the IC flashes.

The IEC of CG2 (Fig. 7b) was only visible in the FA data from the closest sensor site, EE (horizontal distance = 3.4 km from the IEC). Note that the EE FA sensor distorted fast pulses with a ringing artifact in the data, while the slow electric field changes were not distorted. This IEC had a positive slope, which began immediately after the initiating event. The IEC had a point dipole moment of only 9 C m. There were only two enhancing events in this flash, one early and one late. The early enhancing event occurred 19 μs after the initiating event and had a small LogRF power of 0.09 W (−10.6 dBW). This enhancing event started a 75-μs period of approximately constant IEC slope with no FA pulses and only a few weak LogRF pulses. The late enhancing event occurred 30 μs before the first classic IB pulse, and it was also fairly weak (0.19 W, −7.2 dBW). During the last 30 μs before the first classic IB pulse, the number and magnitude of LogRF pulses increased, as in

the IECs described above. As in CG1 the IEC of CG2 had no noticeable FA pulses without LogRF pulses. There were only three FA pulses, the two enhancing events already mentioned and one non-enhancing event that occurred 13 μs before the first classic IB pulse. The main difference between the IEC of CG2 and the other IECs studied herein was that the LogRF pulse identified as the initiating event had the largest power for the time period from initiation through the first classic IB pulse. Thus, except for the fact that both enhancing events had smaller power than the initiating event, the IEC of CG2 was similar to the others studied herein.

6.3. The first classic IB pulse of CG1 and CG2

The first classic IB pulse of CG1 (Fig. 7a) was not a simple bipolar pulse; instead it had two subpulses on the leading-side peak. Also, unlike the weak powers associated with the first classic IB pulse of IC1 and
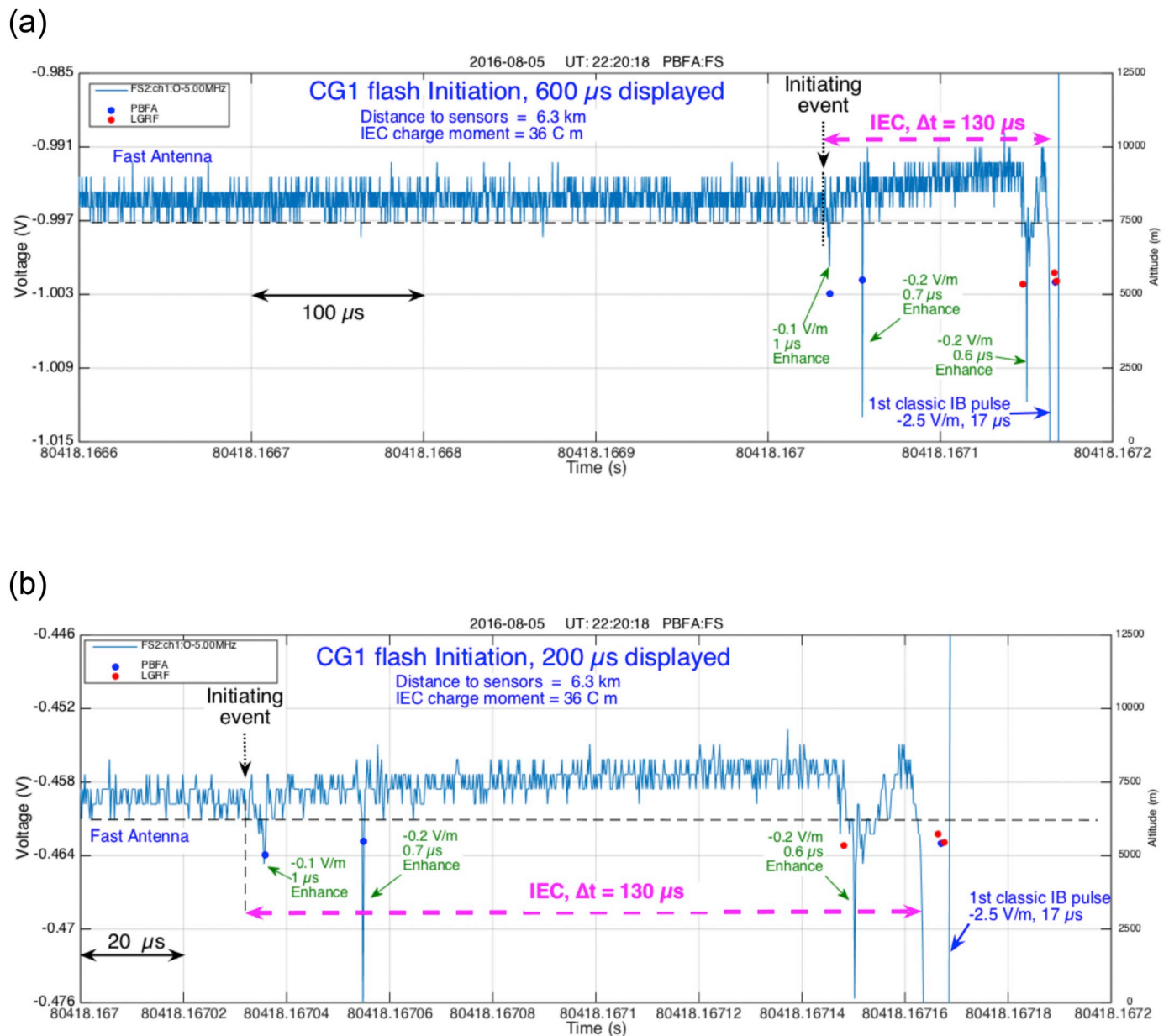
(a)

(b)

Fig. 8. Two additional views of CG2 from Fig. 7a. The time marked "Initiating event" is the time of the first LogRF pulse above background in Fig. 7a. (a) An expanded E-change scale to make the weak IEC easier to see; the time axis has 400 μs added before the 200 μs shown in Fig. 7a to make the IEC easier to see in time. (b) Identical to Fig. 8a in the E-change scale, but only showing the last 200 μs, as in Fig. 7a.

IC2 (Fig. 4a and b), the LogRF power of this IB pulse was 3.0 W (4.8 dBW) and the pulse duration was 7 μs. The peak LogRF power occurred at the local minimum between the two largest subpulses of the classic IB pulse, only 0.4 μs before the largest negative FA value (see vertical dashed line in Fig. 7a).

The first classic IB pulse of CG2 (Fig. 7b) was a simple bipolar pulse, as found for IC1 and IC2, with weak LogRF power (0.32 W, −5.0 dBW), and short duration (2 μs). The bipolar FA pulse had a 2 μs negative leading peak followed by a 13 μs positive overshoot portion; most of the LogRF power occurred during the overshoot. In both CG flashes the first classic IB pulse was followed by a continued sequence of large-amplitude LogRF pulses with almost no coincident FA pulses (outlined in Fig. 7a and b with a dotted rectangle and double question marks). A similar sequence of LogRF pulses, mentioned above, occurred after the *second* classic IB pulse in the IC flashes. As for the IC flashes, the cause of the large number of relatively large LogRF pulses after the first classic IB pulse is unknown.

6.4. Summary: initiation through the first classic IB pulse for CG1 and CG2

Overall, the initiating events of CG1 and CG2 (Fig. 7) were probably positive corona streamers moving upward with weak VHF powers. (The initiating events had VHF powers that were three orders of magnitude weaker than the CG flashes initiated by –NBEs, as described in Rison et al. (2016)). With one exception, the development of the IECs was quite similar to the IEC development of IC1 and IC2, so the same physical mechanisms may be occurring, except the initiating positive streamers moved upward in CG flashes rather than downward (as dictated by the opposite polarity of the thundercloud electric field at negative CG flash initiation). After the initiating event, additional enhancing events during the IEC presumably helped increase the electric field at the ends of the nascent channel and helped increase the conductivity of the nascent channel. We hypothesize that the enhancing events were also positive corona streamers moving upward from the upper end of the nascent leader, but we cannot rule out some sort of

negative breakdown from the lower end of the nascent leader. As in IC1 and IC2, we hypothesize that increased electric field and increased channel conductivity were needed to start the negative breakdown of the first classic IB pulse, which moved downward from the lower end of the nascent leader. The main difference between the IECs of the CG flashes and the IC flashes was that the CG IECs had no noticeable FA pulses without LogRF pulses. We have no explanation for this difference, but we note that three contributing factors might be (1) the much shorter durations of CG IECs giving less time for pulses, (2) the much weaker CG IEC charge moments with perhaps only weaker pulses, and (3) the much shorter reversal distances for CG IECs making pulses harder to detect.

7. Conclusions

We have studied the lightning initiation of two IC flashes and two negative CG flashes by comparing the electromagnetic radiation emitted in two bandwidths, ~0–2.5 MHz and 186–192 MHz. The lower frequency (FA) sensors most easily detect charge motions ≥120 m in length while the higher frequency (LogRF) sensors most easily detect charge motions of ~1.6 m. The flashes chosen were initiated by events whose LogRF powers were smaller, by factors of 10^5 (IC flashes) and 10^3 (CG flashes), than the VHF powers of flashes initiated by NBEs (Rison et al., 2016). We also investigated the events during the IEC (Initial E-Change) of these flashes to see which were enhancing events that contributed to increasing the electric field before the first classic IB pulse. In most lightning flashes the first classic IB pulse is followed by a series of additional IB pulses that, as hypothesized by Clarence and Malan (1957) and Stolzenburg et al. (2013, 2014), increase channel length and conductivity, thereby allowing a negative stepped leader to begin.

A summary of the findings for the four flashes includes the following:

1. A LogRF pulse occurred at the beginning of each flash and was coincident with the beginning of the IEC seen in the FA data. Therefore, this LogRF pulse was caused by the flash initiation event.
2. For three of the four flashes the initiating event did not have a coincident pulse in the FA data, thereby suggesting that most initiating events had relatively short lengths. A related finding was reported by Chapman et al. (2017), in which FA pulses were detected at the beginning of only 28% of 75 IECs.
3. All four of the initiating LogRF pulses had powers < 1 W and durations of ~1 μs, so they were much weaker in power and much shorter in duration than NBEs that initiate flashes (e.g., Rison et al., 2016).
4. The duration of the IECs, or the time between the initiating event and the first classic IB pulse, was 620 and 1790 μs in the IC flashes and 124 and 130 μs in the CG flashes.
5. Numerous LogRF pulses occurred during each IEC, and only a few FA pulses occurred during each IEC. Almost all of the LogRF pulses had durations ≤3 μs while the FA pulses had durations of 1–7 μs.
6. During the IEC, a few of the LogRF pulses were coincident with a noticeable FA pulse, and most of these coincident pairs of FA/ LogRF pulses seemed to cause IEC enhancements, i.e., an increase in the magnitude of the slope of the IEC. No IEC enhancing events occurred in these four flashes without a coincident pair of LogRF and FA pulses. However, we would not be surprised if further studies find IEC enhancements without a coincident FA/LogRF pair because the small amplitudes of some pulses coupled with distance to the closest sensor could make some pulses undetectable.
7. Each flash had 1 or 2 IEC enhancing events soon after initiation; for three flashes the first enhancing event occurred < 20 μs after initiation.
8. Each flash had 1 or 2 IEC enhancing events shortly before the first classic IB pulse. The last enhancing event occurred from 14 μs to 54 μs before the first classic IB pulse.
9. In each flash there was a relatively long time between the early and late enhancing events during which only a few LogRF and FA pulses occurred. During this time the slope of the IEC remained approximately constant. For two of the four flashes, most of the net electric field change of the IEC occurred during this time.
10. The IECs of the two IC flashes had substantial point dipole moments, –520C m and − 770C m, while the IEC dipole moments of the two CG flashes were only 9C m and 36C m.
11. The magnitudes of zero-to-peak FA amplitudes of the first classic IB pulses (range-normalized to 100 km) were 0.3, 1.0, 2.5, and 3.0 V/ m.
12. For three of the four flashes the first classic IB pulse had a simple bipolar waveform (and no subpulses). For those three IB pulses, the LogRF power was ≤ 0.53 W. In the other flash the first classic IB pulse had two subpulses on the leading side of the bipolar waveform and a much larger LogRF power, 3.0 W.

Overall, the findings indicate that after the initiating event, many small-scale events occur during the IEC; together, these events contribute to the production of the first classic IB pulse of the flash. Obviously more flash initiations should be studied in a similar way as the four examples studied herein to determine if the above findings are typical of lightning flash initiations.

We note that the durations of IECs were much longer in IC1 and IC2 than in CG1 and CG2, and the IEC dipole moments before the first classic IB pulse were much bigger for IC1 and IC2 than for CG1 and CG2. These findings are in keeping with prior results for typical flashes in small Florida storms (Marshall et al., 2014; Chapman et al., 2017). These findings indicate that IC flashes may be more difficult to initiate than CG flashes.

Phelps (1974) suggested that lightning initiation would begin with a positive corona streamer, the streamer would produce a dipolar charge distribution that would enhance the electric field at the ends of the streamer path, the enhanced field would cause a second positive corona streamer, etc. The positive streamers would spread out in a conical shape with the axis of the cone parallel to the thundercloud electric field. Phelps (1974) suggested that the series of positive corona streamers would cause "a lowering and concentrating of negative charge" in CG flashes that would increase the net electric field sufficiently to allow negative breakdown to occur.

We speculate that our findings listed above might fit the hypotheses of Phelps (1974) in the following ways:

a. *If* each flash initiation began with a positive corona streamer that ionized a short path in virgin air, *then* the first detected LogRF pulse (duration ~1 μs) in each flash was caused by the short-length positive corona streamer.
b. *If* the strong thundercloud electric field in the vicinity of each initiating event started many subsequent positive corona streamers during the IEC, *then* the many short-duration LogRF pulses detected during the IEC were caused by these subsequent streamers. Meanwhile, most of the physical events that occurred during the IEC were too short and/or too weak to produce noticeable FA pulses or enhance the slope of the IEC.
c. *If* a positive corona streamer or streamer system intermittently either extended former streamers (as suggested by Phelps (1974)) or connected two or more previous streamers, *then* perhaps each IEC enhancing event was caused by such an extension or connection. The FA pulses of the enhancing events might then be more noticeable in the data due to the longer current paths (from extended streamers or multiple connected streamers) and/or due to stronger currents from increased channel conductivity (from multiple streamers passing along the same nascent channel).
d. *If* the IEC created a dipolar charge distribution that enhanced the

thundercloud electric field near the ends of dipole, *then* eventually the net electric field, (i.e., the superposition of the cloud field and the dipole electric field) became sufficient for a negative breakdown of some sort that produced the first classic IB pulse.

Acknowledgements

Funding

Declarations of interest

None.

Appendix A. Appendix

Here we give descriptions of the other two sensors deployed at each sensor site.

A. The Slow Antenna was a calibrated flat-plate *E*-change sensor with a gain of ~0.1 relative to the Fast Antennas and with a relatively long electronic decay time of 1.0 s. The slow antennas were identical to the "ch3 sensors" described in Karunarathne et al. (2013). The sensor bandwidth was 0.16 Hz – 2.6 MHz, so the "characteristic length" of the electromagnetic waves detected by the slow antenna was ≥ 120 m. The 12-bit data were digitized and recorded in the same way as the fast antenna. Since the maximum IEC durations are < 10 ms (Chapman et al., 2017), the slow antenna can give reliable values of the net E-change of all IECs. Slow antenna data can be used to find PBFA locations of fast lightning events (Karunarathne et al., 2013)

B. The dE/dt sensor was a flat-plate antenna that measured the time derivative of electric field (e.g., Weidman and Krider, 1980). Bandwidth was ~ 0–2.5 MHz. Data were digitized at 10 MS/s with a bit depth of 12 and recorded. The dE/dt sensor almost never saturated. With care, dE/dt can be integrated over a short time period to reproduce fast pulses that are identical to the FA data for these pulses, but slower E changes cannot be retrieved. In some cases integrated dE/dt can give a better representation of a small amplitude pulse than the FA or slow antenna. Integrated dE/dt data can also be fed into the TOA algorithm of Karunarathne et al. (2013) to find locations of lightning events.

References

Bils, J.R., Thomson, E.M., Uman, M.A., Mackerras, D., 1988. Electric field pulses in close lightning cloud flashes. J. Geophys. Res. 93 (15), 933–15,940. https://doi.org/10.1029/JD093iD12p15933.

Chapman, R., Marshall, T., Karunarathne, S., Stolzenburg, M., 2017. Initial electric field changes of lightning flashes in two thunderstorms. J. Geophys. Res. Atmos. 122, 3718–3732. https://doi.org/10.1002/2016JD025859.

Clarence, N.D., Malan, D.J., 1957. Preliminary discharge processes in lightning flashes to ground. Q. J. R. Meteorol. Soc. 83, 161–172.

Dawson, G.A., Winn, W.P., 1965. A model for streamer propagation. Z. Phys. 183, 159–171.

Griffiths, R.F., Phelps, C.T., 1976. A model of lightning initiation arising from positive corona streamer development. J. Geophys. Res. 31, 3671–3676.

Hamlin, T., 2004. The New Mexico Tech Lightning Mapping Array. PhD dissertation. New Mexico Institute of Mining and Technology, Socorro, NM.

Karunarathne, S., Marshall, T.C., Stolzenburg, M., Karunarathna, N., Vickers, L.E., Warner, T.A., Orville, R.E., 2013. Locating initial breakdown pulses using electric field change network. J. Geophys. Res. Atmos. 118, 7129–7141. https://doi.org/10.1002/jgrd.50441.

Kitagawa, N., Brook, M., 1960. A comparison of intracloud and cloud-to-ground lightning discharges. J. Geophys. Res. 65 (4), 1189–1201.

Krehbiel, Paul, Peterson, Danyal, da Silva, Caitano, 2017. Fast breakdown as coronal/ionization waves? In: American Geophysical Union Fall Meeting, Abstract AE12A-06.

Marshall, T., Stolzenburg, M., Karunarathne, S., Cummer, S., Lu, G., Betz, H.-D., Briggs, M., Connaughton, V., Xiong, S., 2013. Initial breakdown pulses in intracloud lightning flashes and their relation to terrestrial gamma ray flashes. J. Geophys. Res. Atmos. 118 (10), 907–10,925. https://doi.org/10.1002/jgrd.50866.

Marshall, T., Stolzenburg, M., Karunarathna, N., Karunarathne, S., 2014. Electromagnetic activity before initial breakdown pulses of lightning. J. Geophys. Res. Atmos. 119 (12), 558–12,574. https://doi.org/10.1002/2014JD022155.

Nag, A., DeCarlo, B.A., Rakov, V.A., 2009. Analysis of microsecond and submicrosecond-scale electric field pulses produced by cloud and ground lightning discharges. Atmos. Res. 91, 316.

Phelps, C.T., 1971. Field-enhanced propagation of corona streamers. J. Geophys. Res. 76, 5799–5806.

Phelps, C.T., 1974. Positive streamers system intensification and its possible role in lightning initiation. J. Atmos. Terr. Phys. 36, 103–111.

Rakov, V.A., Uman, M.A., 2003. Lightning, Physics and Effects. Cambridge Univ. Press, Cambridge, U. K.

Rison, W., et al., 2016. Observations of narrow bipolar events reveal how lightning is initiated in thunderstorms. vol. 7, 10721. https://doi.org/10.1038/ncomms10721.

Shao, X.M., Krehbiel, P.R., 1996. The spatial and temporal development of intracloud lightning. J. Geophys. Res. 101, 26641–26668.

Stolzenburg, M., Marshall, T.C., Karunarathne, S., Karunarathna, N., Vickers, L.E., Warner, T.A., Orville, R.E., Betz, H.-D., 2013. Luminosity of initial breakdown in lightning. J. Geophys. Res. Atmos. 118. https://doi.org/10.1002/jgrd.50276.

Stolzenburg, M., Marshall, T.C., Karunarathne, S., Karunarathna, N., Orville, R.E., 2014. Leader observations during the initial breakdown stage of a lightning flash. J. Geophys. Res. Atmos. 119, 12,198–12,221. https://doi.org/10.1002/2014JD021994.

Uman, M.A., McLain, D.K., Krider, E.P., 1975. The electromagnetic radiation from a finite antenna. Am. J. Phys. 43, 33–38.

Weidman, C.D., Krider, E.P., 1979. The radiation field waveforms produced by intracloud lightning discharge processes. J. Geophys. Res. 84 (C6), 3159–3164.

Weidman, C.D., Krider, E.P., 1980. Sub-microsecond risetimes in lightning return-stroke fields. Geophys. Res. Lett. 7, 955–958.

Willett, J.C., Bailey, J.C., Krider, E.P., 1989. A class of unusual lightning electric field waveforms with very strong high-frequency radiation. J. Geophys. Res. 94 (D13), 16,255–16,267. https://doi.org/10.1029/JD094iD13p16255.